

February 8, 2021

Beauty meson decays to charmonium-like states at LHCb

Tatiana Ovsianikova[†] on behalf of the LHCb collaboration

*Institute for Theoretical and Experimental Physics, NRC Kurchatov Institute,
B. Cheremushkinskaya 25, Moscow, 117218, Russia.*

Abstract

The decays $B_s^0 \rightarrow J/\psi \pi^+ \pi^- K^+ K^-$ are studied using a data set corresponding to an integrated luminosity of 9 fb^{-1} , collected with the LHCb detector in proton-proton collisions at centre-of-mass energies of 7, 8 and 13 TeV. The decays $B_s^0 \rightarrow J/\psi K^{*0} \bar{K}^{*0}$ and $B_s^0 \rightarrow \chi_{c1}(3872) K^+ K^-$, where the $K^+ K^-$ pair does not originate from a ϕ meson, are observed for the first time. Precise measurements of the ratios of branching fractions between intermediate $\chi_{c1}(3872)\phi$, $J/\psi K^{*0} \bar{K}^{*0}$, $\psi(2S)\phi$ and $\chi_{c1}(3872)K^+K^-$ states are reported. A structure, denoted as $X(4740)$, is observed in the $J/\psi \phi$ mass spectrum with a significance in excess of 5.3 standard deviation. In addition, the most precise single measurement of the mass of the B_s^0 meson is performed.

Talk given at 23th International Conference in Quantum Chromodynamics (QCD 20, 35th anniversary), 27 - 30 November 2020, Montpellier - FR

[†]E-mail: Tatiana.Ovsianikova@cern.ch

1 Introduction

Decays of beauty hadrons to final states with charmonia provide a unique laboratory to study the properties of charmonia and charmonium-like states. A plethora of new charmonium-like states has been observed in the decays of beauty mesons, such as the $\chi_{c1}(3872)$ meson [1] and numerous tetraquark candidates [2–11]. The nature of many exotic charmonium-like candidates remains unclear. A comparison of production rates with respect to those of conventional charmonium states in decays of beauty hadrons can shed light on their production mechanisms.

The reported results are based on the data samples collected by the LHCb experiment in proton-proton (pp) collisions at centre-of-mass energies $\sqrt{s} = 7, 8$ and 13 TeV between 2011 and 2018.

2 Study of the $B^+ \rightarrow J/\psi \pi^+ \pi^- K^+$ decays.

Candidate $B^+ \rightarrow J/\psi \pi^+ \pi^- K^+$ decays are reconstructed using the $J/\psi \rightarrow \mu^+ \mu^-$ decay mode. A loose pre-selection is applied, followed by a multivariate classifier based on a decision tree with gradient boosting [12].

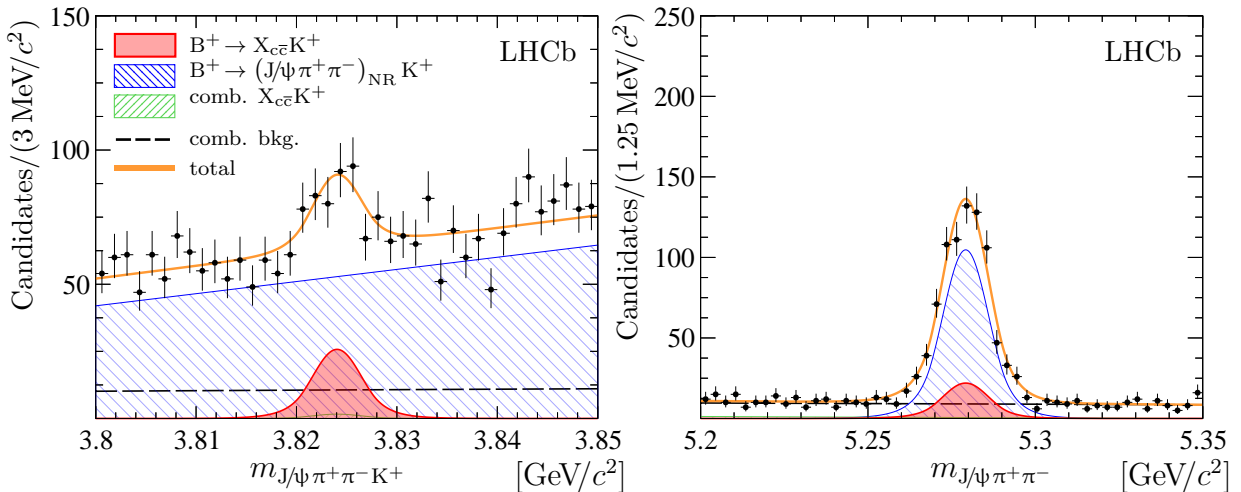


Figure 1: Distributions of the (left) $J/\psi \pi^+ \pi^- K^+$ and (right) $J/\psi \pi^+ \pi^-$ mass for the selected $B^+ \rightarrow \psi_2(3823)K^+$ candidates (points with error bars) [12, 13].

The yields for the $B^+ \rightarrow J/\psi \pi^+ \pi^- K^+$ decays via intermediate $\chi_{c1}(3872) \rightarrow J/\psi \pi^+ \pi^-$, $\psi_2(3823) \rightarrow J/\psi \pi^+ \pi^-$ and $\psi(2S) \rightarrow J/\psi \pi^+ \pi^-$ chains are determined using a simultaneous unbinned extended maximum-likelihood fit to the $J/\psi \pi^+ \pi^- K^+$ mass and the $J/\psi \pi^+ \pi^-$ mass distributions. The fit is performed in the three non-overlapping regions around the $\psi_2(3823)$, $\chi_{c1}(3872)$ and $\psi(2S)$ masses. To improve the resolution on the $J/\psi \pi^+ \pi^-$ mass and to eliminate a small correlation between $m_{J/\psi \pi^+ \pi^- K^+}$ and $m_{J/\psi \pi^+ \pi^-}$ variables, the $m_{J/\psi \pi^+ \pi^-}$ variable is computed using a kinematic fit that constrains the mass of the B^+ candidate to its known value [14]. The signal yields are determined to be 137 ± 26 events for the $B^+ \rightarrow \psi_2(3823)K^+$ decay which correspond to statistical significance above 5.1σ . The fit to the mass distribution for the signal channel are shown in figure 1. Also the significant signal yield is observed for the $B^+ \rightarrow \chi_{c1}(3872)K^+$ decay 4230 ± 70 events which

allows the precise determination of the parameters of the $\chi_{c1}(3872)$ state, in particular for the first time the non-zero width for the $\chi_{c1}(3872)$ state is observed with significance more than 5 standard deviations

$$\Gamma_{\chi_{c1}(3872)} = 0.96_{-0.18}^{+0.19} \pm 0.21 \text{ MeV},$$

where the first uncertainty is statistical and the second is systematic. The value of the Breit–Wigner width agrees well with the value from the analysis of a large sample of $\chi_{c1}(3872) \rightarrow J/\psi \pi^+ \pi^-$ decays from the inclusive decays of beauty hadrons [15]. The improved upper limit for the width of the $\psi_2(3823)$ meson is found to be $\Gamma_{\psi_2(3823)} < 5.2 (6.6) \text{ MeV}$ for 90 (95)% C.L. The mass differences between $\psi_2(3823)$, $\chi_{c1}(3872)$ and $\psi(2S)$ mesons, $\delta m_X^Y \equiv m_X - m_Y$, are measured to be

$$\begin{aligned} \delta m_{\psi_2(3823)}^{\chi_{c1}(3872)} &= 47.50 \pm 0.53 \pm 0.13 \text{ MeV}/c^2, \\ \delta m_{\psi(2S)}^{\psi_2(3823)} &= 137.98 \pm 0.53 \pm 0.14 \text{ MeV}/c^2, \\ \delta m_{\psi(2S)}^{\psi_2(3823)} &= 185.49 \pm 0.06 \pm 0.03 \text{ MeV}/c^2, \end{aligned}$$

where the first uncertainty is statistical and the second is systematic. Using the measured mass difference the binding energy of the $\chi_{c1}(3872)$ state is calculated to be $\delta E = 0.12 \pm 0.13 \text{ MeV}$. It is consistent with zero within uncertainties, that are currently dominated by the uncertainty for the charged and neutral kaon mass measurements.

The measured yields of the $B^+ \rightarrow \chi_{c1}(3872)K^+$, $B^+ \rightarrow \psi_2(3823)K^+$ and $B^+ \rightarrow \psi(2S)K^+$ signal decays allow for a precise determination of the ratios of the branching fractions:

$$\begin{aligned} \frac{\mathcal{B}_{B^+ \rightarrow \psi_2(3823)K^+} \times \mathcal{B}_{\psi_2(3823) \rightarrow J/\psi \pi^+ \pi^-}}{\mathcal{B}_{B^+ \rightarrow \chi_{c1}(3872)K^+} \times \mathcal{B}_{\chi_{c1}(3872) \rightarrow J/\psi \pi^+ \pi^-}} &= (3.56 \pm 0.67 \pm 0.11) \times 10^{-2}, \\ \frac{\mathcal{B}_{B^+ \rightarrow \psi_2(3823)K^+} \times \mathcal{B}_{(\psi_2(3823) \rightarrow J/\psi \pi^+ \pi^-)}}{\mathcal{B}_{B^+ \rightarrow \psi(2S)K^+} \times \mathcal{B}_{\psi(2S) \rightarrow J/\psi \pi^+ \pi^-}} &= (1.31 \pm 0.25 \pm 0.04) \times 10^{-3}, \\ \frac{\mathcal{B}_{B^+ \rightarrow \chi_{c1}(3872)K^+} \times \mathcal{B}_{\chi_{c1}(3872) \rightarrow J/\psi \pi^+ \pi^-}}{\mathcal{B}_{B^+ \rightarrow \psi(2S)K^+} \times \mathcal{B}_{\psi(2S) \rightarrow J/\psi \pi^+ \pi^-}} &= (3.69 \pm 0.07 \pm 0.06) \times 10^{-2}. \end{aligned}$$

3 Study of the $B_s^0 \rightarrow J/\psi \pi^+ \pi^- K^+ K^-$ decays

The $B_s^0 \rightarrow J/\psi \pi^+ \pi^- K^+ K^-$ decays are reconstructed using selection criteria based on kinematics, particle identification and topology [16]. The yields of $B_s^0 \rightarrow J/\psi \pi^+ \pi^- K^+ K^-$ decays via intermediate $\psi(2S) \rightarrow J/\psi \pi^+ \pi^-$ and $\chi_{c1}(3872) \rightarrow J/\psi \pi^+ \pi^-$ chains are determined using a three-dimensional unbinned extended maximum-likelihood fit to the $J/\psi \pi^+ \pi^- K^+ K^-$, $J/\psi \pi^+ \pi^-$ and $K^+ K^-$ mass distributions. The fit is performed simultaneously in two separate regions corresponding to $B_s^0 \rightarrow \chi_{c1}(3872)\phi$ and $B_s^0 \rightarrow \psi(2S)\phi$ signals as described above.

The observed signal yield for the $B_s^0 \rightarrow \chi_{c1}(3872)\phi$ decays is found to be 154 ± 15 events which corresponds to the statistical significance more than 10σ deviation. The fit to the mass distribution for the signal channel are shown in figure 2. Using the obtained signal yields for $B_s^0 \rightarrow \chi_{c1}(3872)\phi$ and $B_s^0 \rightarrow \psi(2S)\phi$ channels and corresponding efficiency ratio the following branching fraction is calculated:

$$\frac{\mathcal{B}_{B_s^0 \rightarrow \chi_{c1}(3872)\phi} \times \mathcal{B}_{\chi_{c1}(3872) \rightarrow J/\psi \pi^+ \pi^-}}{\mathcal{B}_{B_s^0 \rightarrow \psi(2S)\phi} \times \mathcal{B}_{\psi(2S) \rightarrow J/\psi \pi^+ \pi^-}} = (2.42 \pm 0.23 \pm 0.07) \times 10^{-2}.$$

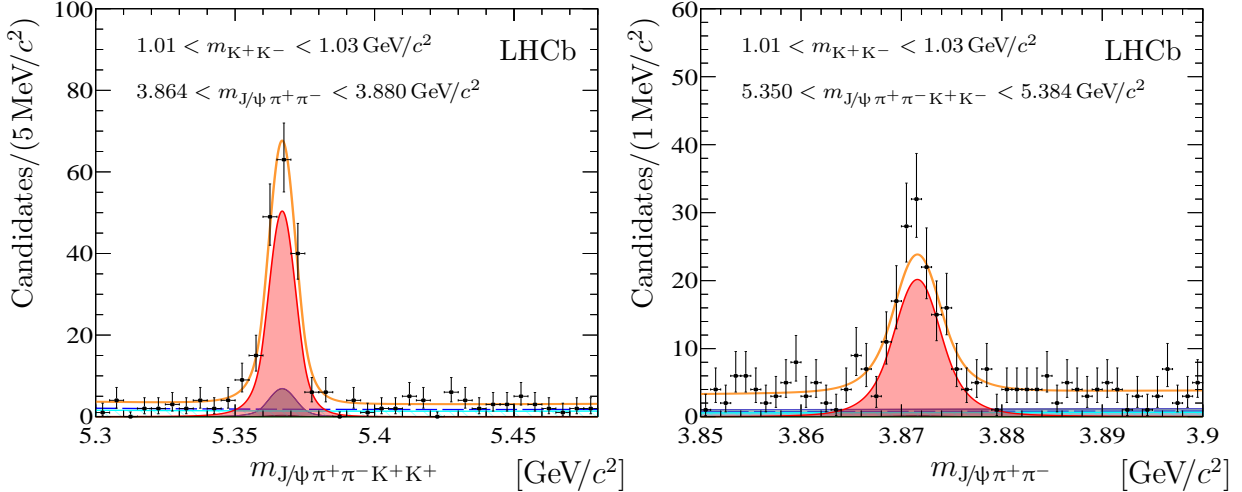


Figure 2: Distributions of the (left) $J/\psi \pi^+ \pi^- K^+ K^-$ and (right) $J/\psi \pi^+ \pi^-$ mass for selected $B_s^0 \rightarrow \chi_{c1}(3872)\phi$ candidates (points with error bars) [16]. The red filled area corresponds to the $B_s^0 \rightarrow \chi_{c1}(3872)\phi$ signal. The orange line is the total fit.

The obtained value is found to be in a good agreement with the recent result by the CMS collaboration [17] but is more precise.

The decay $B_s^0 \rightarrow \chi_{c1}(3872)K^+K^-$ where the K^+K^- pair does not originate from a ϕ meson, is studied using a sample of selected $B_s^0 \rightarrow J/\psi \pi^+ \pi^- K^+ K^-$ signal decays. A two-dimensional unbinned extended maximum-likelihood fit is performed to the $J/\psi \pi^+ \pi^-$ and $J/\psi \pi^+ \pi^- K^+ K^-$ mass distributions. The yield of the $B_s^0 \rightarrow \chi_{c1}(3872)K^+K^-$ signal decays is 378 ± 33 , that is significantly large than the yield of the $B_s^0 \rightarrow \chi_{c1}(3872)\phi$ decays, indicating a large $B_s^0 \rightarrow \chi_{c1}(3872)K^+K^-$ contribution. The background-subtracted and efficiency-corrected K^+K^- mass distribution of the $B_s^0 \rightarrow \chi_{c1}(3872)K^+K^-$ candidates is shown in figure 3. The K^+K^- mass distribution for $m_{K^+K^-} > 1.1$ GeV/c^2 region cannot be described by phase-space shape, and possibly contains contributions from the $f_0(980)$, $f_2(1270)$, $f_0(1370)$ and $f_2'(1520)$ resonances decaying to a pair of kaons, as has been observed in $B_s^0 \rightarrow J/\psi K^+K^-$ decays [18, 19]. Therefore a component that accounts for non-resonant $B_s^0 \rightarrow \chi_{c1}(3872)K^+K^-$ decays and decays via broad high-mass K^+K^- intermediate states, modelled by a product of a phase-space function for three-body $B_s^0 \rightarrow \chi_{c1}(3872)K^+K^-$ decays and a third-order polynomial function. An amplitude analysis of a larger data sample would be required to properly disentangle individual contributions. However, a narrow ϕ component can be separated from the non- ϕ components using an unbinned maximum-likelihood fit to the background-subtracted and efficiency-corrected K^+K^- mass distribution. The fraction of the $B_s^0 \rightarrow \chi_{c1}(3872)K^+K^-$ signal component is found to be $(38.9 \pm 4.9)\%$ and further propagated to the branching fraction ratio:

$$\frac{\mathcal{B}_{B_s^0 \rightarrow \chi_{c1}(3872)(K^+K^-)_{\text{non-}\phi}}}{\mathcal{B}_{B_s^0 \rightarrow \chi_{c1}(3872)\phi} \times \mathcal{B}_{\phi \rightarrow K^+K^-}} = 1.57 \pm 0.32 \pm 0.12.$$

The yield of $B_s^0 \rightarrow J/\psi K^{*0} \bar{K}^{*0}$ decays is determined using a three-dimensional unbinned extended maximum-likelihood fit to the $J/\psi \pi^+ \pi^- K^+ K^-$, $K^- \pi^+$ and $K^+ \pi^-$ mass distributions. Using the obtained signal yields and the corresponding efficiency ratio the branching

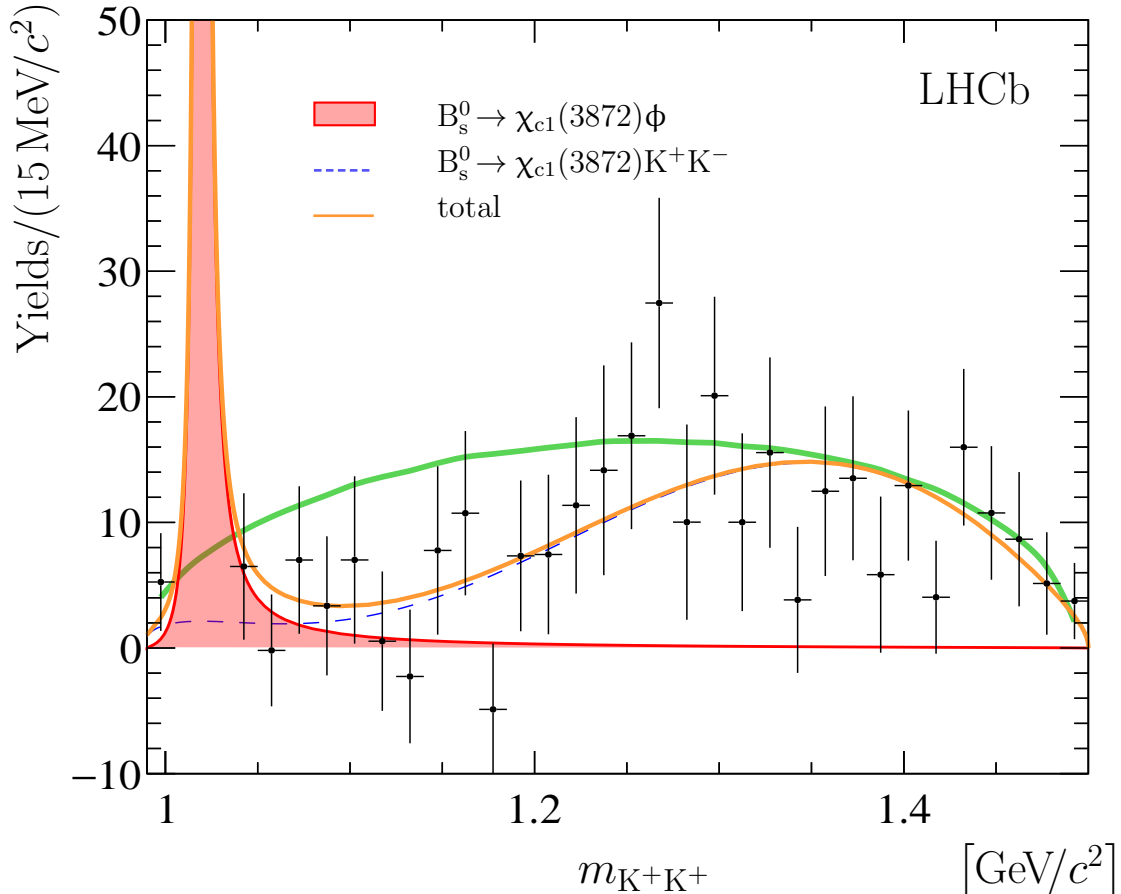


Figure 3: Background-subtracted K^+K^- mass distribution for selected $B_s^0 \rightarrow \chi_{c1}(3872)K^+K^-$ candidates (points with error bars) [16]. A fit, described in the text, is overlaid. The red filled area corresponds to the $B_s^0 \rightarrow \chi_{c1}(3872)\phi$ signal. The blue dashed line corresponds to the $B_s^0 \rightarrow \chi_{c1}(3872)K^+K^-$ component. The orange line is the total fit. The expectation for phase-space simulated decays is shown as a green solid line.

fraction ratio is calculated:

$$\frac{\mathcal{B}_{B_s^0 \rightarrow J/\psi K^{*0} \bar{K}^{*0}} \times \mathcal{B}_{K^{*0} \rightarrow K^+ \pi^-}^2}{\mathcal{B}_{B_s^0 \rightarrow \psi(2S)\phi} \times \mathcal{B}_{\psi(2S) \rightarrow J/\psi \pi^+ \pi^-} \times \mathcal{B}_{\phi \rightarrow K^+ K^-}} = 1.22 \pm 0.03 \pm 0.04.$$

The $J/\psi\phi$ spectrum is studied using the $B_s^0 \rightarrow J/\psi\pi^+\pi^-\phi$ decays. The $B_s^0 \rightarrow J/\psi\pi^+\pi^-\phi$ candidates are determined with two-dimensional unbinned extended maximum-likelihood fit to the $J/\psi\pi^+\pi^-K^-K^+$ and K^+K^- mass distributions. The background-subtracted $J/\psi\phi$ mass spectrum of selected $B_s^0 \rightarrow J/\psi\pi^+\pi^-\phi$ decays shown in figure 4. It shows a prominent structure at a mass around $4.74 \text{ GeV}/c^2$. No such structure is seen if the K^+K^- mass is restricted to the region of $1.06 < m_{K^+K^-} < 1.15 \text{ GeV}/c^2$. This structure cannot be explained by $B_s^0 \rightarrow \chi_{c1}(3872)\phi$ and $B_s^0 \rightarrow \psi(2S)\phi$ decays via a narrow intermediate $\psi(2S)$ and $\chi_{c1}(3872)$ resonance since contributions from these decays are explicitly vetoed. No sizeable contributions from decays via other narrow charmonium states are observed in the background-subtracted $J/\psi\pi^+\pi^-$ mass spectrum. The $\phi\pi^+\pi^-$ spectrum exhibits significant deviations from the phase-space distribution, indicating possible presence of excited ϕ states, referred

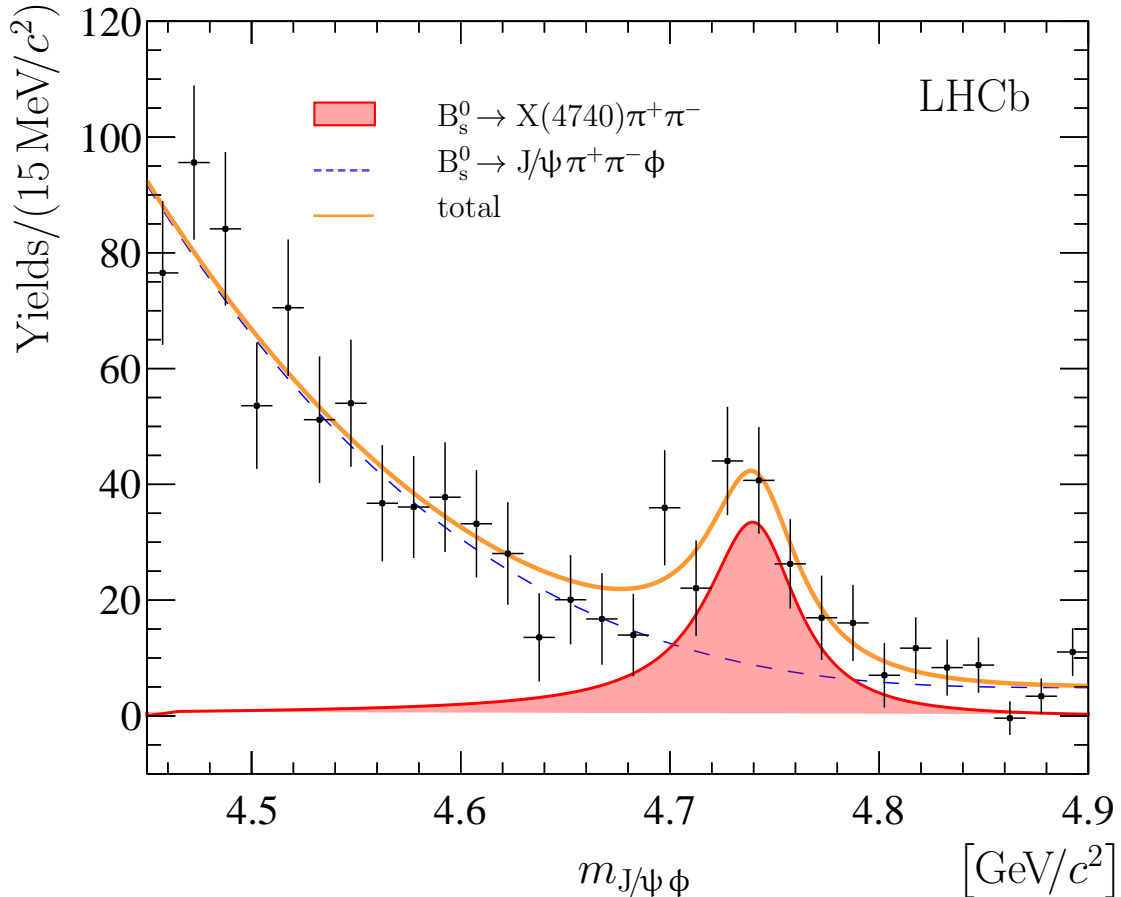


Figure 4: Background-subtracted $J/\psi \phi$ mass distribution for selected $B_s^0 \rightarrow J/\psi \pi^+ \pi^- \phi$ candidates (points with error bars) [16]. The red filled area corresponds to the $B_s^0 \rightarrow X(4740) \pi^+ \pi^-$ signal. The orange line is the total fit.

to as ϕ^* states hereafter. The decays $B_s^0 \rightarrow J/\psi \phi^*$ via intermediate $\phi(1680)$, $\phi(1850)$ or $\phi(2170)$ states [14] are studied using simulated samples and no peaking structures are observed. Under the assumption that the observed structure, referred to as $X(4740)$ hereafter, has a resonant nature, its mass and width are determined through an unbinned extended maximum-likelihood fit to the background-subtracted $J/\psi \phi$ mass distribution in the range $4.45 < m_{J/\psi \phi} < 4.90 \text{ GeV}/c^2$. The fit result is superimposed in figure 4. The obtained signal yield is 175 ± 39 events and corresponds to a statistical significance above the 5.3σ . The mass and width for the $X(4740)$ state are found to be

$$\begin{aligned} m_{X(4740)} &= 4741 \pm 6 \pm 6 \text{ GeV}/c^2, \\ \Gamma_{X(4740)} &= 53 \pm 15 \pm 11 \text{ MeV}. \end{aligned}$$

The observed parameters qualitatively agree with those of the $\chi_{c1}(4700)$ state observed by the LHCb collaboration in an amplitude analysis of $B^+ \rightarrow J/\psi \phi K^+$ decays [8, 9]. The obtained mass also agrees with the one expected for the $2^{++} c\bar{s}c\bar{s}$ tetraquark state [20].

The B_s^0 decays to the $J/\psi \pi^+ \pi^- K^+ K^-$ final states characterize the relatively small energy release allowing precise measurement of the B_s^0 meson mass. The mass of the B_s^0 meson is determined from an unbinned extended maximum-likelihood fit to the $\psi(2S)K^+K^-$ mass distribution for a sample of $B_s^0 \rightarrow J/\psi \pi^+ \pi^- K^+ K^-$ decays with $m_{K^+K^-} < 1.06 \text{ GeV}/c^2$

and with the $J/\psi \pi^+ \pi^-$ mass within a narrow region around the known mass of the $\psi(2S)$ meson. The improvement in the B_s^0 mass resolution and significant decrease of the systematic uncertainties is achieved by imposing a constraint on the reconstructed mass of the $J/\psi \pi^+ \pi^-$ system to a known mass of the $\psi(2S)$ meson [14, 21]. The measured value of the B_s^0 meson mass is found to be

$$m_{B_s^0} = 5366.98 \pm 0.07 \pm 0.13 \text{ MeV}/c^2,$$

that is the most precise single measurement of this quantity. This result is combined with other precise measurements by the LHCb collaboration using $B_s^0 \rightarrow J/\psi \phi$ [22], $B_s^0 \rightarrow J/\psi \phi \phi$ [23], $B_s^0 \rightarrow \chi_{c2} K^+ K^-$ [24] and $B_s^0 \rightarrow J/\psi p \bar{p}$ [25] decays. The combined mass is calculated accounting for correlations of systematic uncertainties between the measurements. The LHCb average for the mass of the B_s^0 meson is found to be

$$m_{B_s^0}^{\text{LHCb}} = 5366.94 \pm 0.08 \pm 0.09 \text{ MeV}/c^2.$$

The comparison with previous measurements is presented in figure 5.

4 Conclusions

A study of B-meson decays $B^+ \rightarrow J/\psi \pi^+ \pi^- K^+$ and $B_s^0 \rightarrow J/\psi \pi^+ \pi^- K^+ K^-$ is made using pp collision data corresponding to an integrated luminosity of 1, 2 and 6 fb^{-1} , collected with the LHCb detector at centre-of-mass energies of 7, 8 and 13 TeV, respectively [12, 16]. The reported results include the first observation of the non-zero width of the $\chi_{c1}(3872)$ state; the most precise measurement of the masses of the $\chi_{c1}(3872)$ and $\psi_2(3823)$ states; the first observation of the $\psi_2(3823) \rightarrow J/\psi \pi^+ \pi^-$, $B^+ \rightarrow \psi_2(3823) K^+$, $B_s^0 \rightarrow \chi_{c1}(3872) (K^+ K^-)_{\text{non-}\phi}$ and $B_s^0 \rightarrow J/\psi K^{*0} \bar{K}^{*0}$ decays; the most precise measurement of the ratios of branching fractions of the B^+ and B_s^0 mesons into the final states with $\chi_{c1}(3823)$ and $\psi_2(3823)$ particles; the most precise single measurement of the B_s^0 meson mass and an observation of a new structure, denoted as a $X(4740)$ state, in the $J/\psi \phi$ mass spectrum.

Acknowledgments

I would like to express my gratitude to the QCD20 organizers for the great conference. Also, I'm thankful for my colleagues from LHCb collaboration who helped with preparation of this talk.

References

- [1] Belle collaboration, S.-K. Choi *et al.*, *Observation of a narrow charmoniumlike state in exclusive $B^\pm \rightarrow K^\pm \pi^+ \pi^- J/\psi$ decays*, Phys. Rev. Lett. **91** (2003) 262001, arXiv:hep-ex/0309032.
- [2] Belle collaboration, S. K. Choi *et al.*, *Observation of a resonance-like structure in the $\pi^\pm \psi'$ mass distribution in exclusive $B \rightarrow K \pi^\pm \psi'$ decays*, Phys. Rev. Lett. **100** (2008) 142001, arXiv:0708.1790.

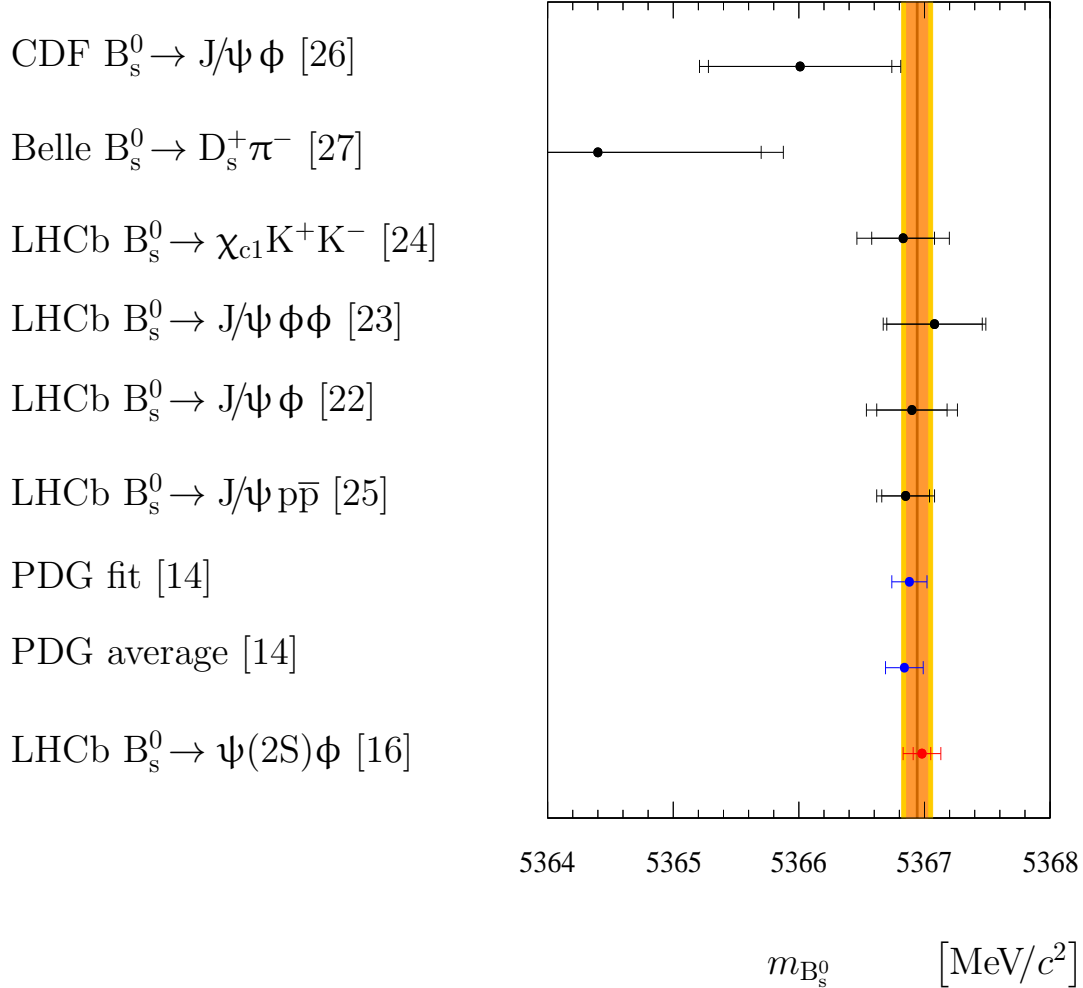


Figure 5: Compilation of the measurements of the B_s^0 meson mass. The inner error bars indicate the statistical uncertainty, and the outer error bars correspond to quadratic sum of statistic and systematic uncertainties. The band represents the value and the uncertainty on the average of LHCb measurements.

- [3] Belle collaboration, R. Mizuk *et al.*, *Dalitz analysis of $B \rightarrow K \pi^+ \psi'$ decays and the $Z(4430)^+$* , Phys. Rev. **D80** (2009) 031104, [arXiv:0905.2869](#).
- [4] Belle collaboration, K. Chilikin *et al.*, *Experimental constraints on the spin and parity of the $Z(4430)^+$* , Phys. Rev. **D88** (2013) 074026, [arXiv:1306.4894](#).
- [5] LHCb collaboration, R. Aaij *et al.*, *Observation of the resonant character of the $Z(4430)^-$ state*, Phys. Rev. Lett. **112** (2014) 222002, [arXiv:1404.1903](#).
- [6] LHCb collaboration, R. Aaij *et al.*, *Model-independent confirmation of the $Z(4430)^-$ state*, Phys. Rev. **D92** (2015) 112009, [arXiv:1510.01951](#).
- [7] LHCb collaboration, R. Aaij *et al.*, *Evidence for exotic hadron contributions to $\Lambda_b^0 \rightarrow J/\psi p \pi^-$ decays*, Phys. Rev. Lett. **117** (2016) 082003, [arXiv:1606.06999](#).

- [8] LHCb collaboration, R. Aaij *et al.*, *Observation of exotic $J/\psi\phi$ structures from amplitude analysis of $B^+ \rightarrow J/\psi\phi K^+$ decays*, Phys. Rev. Lett. **118** (2017) 022003, arXiv:1606.07895.
- [9] LHCb collaboration, R. Aaij *et al.*, *Amplitude analysis of $B^+ \rightarrow J/\psi\phi K^+$ decays*, Phys. Rev. **D95** (2017) 012002, arXiv:1606.07898.
- [10] LHCb collaboration, R. Aaij *et al.*, *Evidence for a $\eta_c(1S)\pi^-$ resonance in $B^0 \rightarrow \eta_c(1S)K^+\pi^-$ decays*, Eur. Phys. J. **C78** (2018) 1019, arXiv:1809.07416.
- [11] LHCb collaboration, R. Aaij *et al.*, *Model-independent observation of exotic contributions to $B^0 \rightarrow J/\psi K^+\pi^-$ decays*, Phys. Rev. Lett. **122** (2019) 152002, arXiv:1901.05745.
- [12] LHCb collaboration, R. Aaij *et al.*, *Study of the $\psi_2(3823)$ and $\chi_{c1}(3872)$ states in $B^+ \rightarrow (J/\psi\pi^+\pi^-)K^+$ decays*, JHEP **08** (2020) 123, arXiv:2005.13422.
- [13] D. Pereima, *Search for new decays of beauty particles at the LHCb experiment*, PhD thesis, NRC Kurchatov Institute - ITEP, Moscow, 2020, CERN-THESIS-2020-204.
- [14] Particle Data Group, P. A. Zyla *et al.*, *Review of particle physics*, Prog. Theor. Exp. Phys. **2020** (2020) 083C01.
- [15] LHCb collaboration, R. Aaij *et al.*, *Study of the line shape of the $\chi_{c1}(3872)$ meson*, arXiv:2005.13419, to appear in Phys. Rev. D.
- [16] LHCb collaboration, R. Aaij *et al.*, *Study of $B_s^0 \rightarrow J/\psi\pi^+\pi^-K^+K^-$ decays*, arXiv:2011.01867, to appear in JHEP.
- [17] CMS collaboration, A. M. Sirunyan *et al.*, *Observation of the $B_s^0 \rightarrow X(3872)\phi$ decay*, Phys. Rev. Lett. **125** (2020) 152001, arXiv:2005.04764.
- [18] LHCb collaboration, R. Aaij *et al.*, *Amplitude analysis and branching fraction measurement of $\bar{B}_s^0 \rightarrow J/\psi K^+K^-$* , Phys. Rev. **D87** (2013) 072004, arXiv:1302.1213.
- [19] LHCb collaboration, R. Aaij *et al.*, *Resonances and CP-violation in B_s^0 and $\bar{B}_s^0 \rightarrow J/\psi K^+K^-$ decays in the mass region above the $\phi(1020)$* , JHEP **08** (2017) 037, arXiv:1704.08217.
- [20] D. Ebert, R. N. Faustov, and V. O. Galkin, *Excited heavy tetraquarks with hidden charm*, Eur. Phys. J. **C58** (2008) 399, arXiv:0808.3912.
- [21] KEDR collaboration, V. V. Anashin *et al.*, *Final analysis of KEDR data on J/ψ and $\psi(2S)$ masses*, Phys. Lett. **B749** (2015) 50.
- [22] LHCb collaboration, R. Aaij *et al.*, *Measurement of b-hadron masses*, Phys. Lett. **B708** (2012) 241, arXiv:1112.4896.
- [23] LHCb collaboration, R. Aaij *et al.*, *Observation of the $B_s^0 \rightarrow J/\psi\phi\phi$ decay*, JHEP **03** (2016) 040, arXiv:1601.05284.
- [24] LHCb collaboration, R. Aaij *et al.*, *Observation of the decay $\bar{B}_s^0 \rightarrow \chi_{c2}K^+K^-$* , JHEP **08** (2018) 191, arXiv:1806.10576.

- [25] LHCb collaboration, R. Aaij *et al.*, *Observation of $B_{(s)}^0 \rightarrow J/\psi p\bar{p}$ decays and precision measurements of the $B_{(s)}^0$ masses*, Phys. Rev. Lett. **122** (2019) 191804, [arXiv:1902.05588](#).
- [26] CDF collaboration, D. Acosta *et al.*, *Measurement of b hadron masses in exclusive J/ψ decays with the CDF detector*, Phys. Rev. Lett. **96** (2006) 202001, [arXiv:hep-ex/0508022](#).
- [27] Belle collaboration, R. Louvot *et al.*, *Measurement of the decay $B_s^0 \rightarrow D_s^- \pi^+$ and evidence for $B_s^0 \rightarrow D_s^\pm K^\mp$ in e^+e^- annihilation at $\sqrt{s} \sim 10.87$ GeV*, Phys. Rev. Lett. **102** (2009) 021801, [arXiv:0809.2526](#).